Planta (2007) 225:1221–1231
DOI 10.1007/s00425-006-0432-8

ORIGINAL PAPER

The ScFRK2 MAP kinase kinase kinase from *Solanum chacoense* affects pollen development and viability

Martin O'Brien · Madoka Gray-Mitsumune · Christelle Kapfer · Charles Bertrand · Daniel P. Matton

Received: 9 September 2006 / Accepted: 16 October 2006 / Published online: 14 November 2006

Abstract We have previously described the FERTILIZATION-RELATED KINASE 2 (ScFRK2), a MAP kinase kinase kinase from *Solanum chacoense* that is predominantly expressed in reproductive tissues. Overexpression of the *ScFRK2* gene modifies the cell fate of ovule initials and induces homeotic transformation of ovules into carpelloid structures. Since the *ScFRK2* gene is normally expressed also in anthers, we now further our observations on the effect of *ScFRK2* overexpression in male reproductive structures. Although *ScFRK2* mRNA levels detected by RNA blot were relatively constant during early anther development, there was a dramatic change in tissue distribution of *ScFRK2* mRNA when detected by in situ RNA hybridization. In the young anther, *ScFRK2* mRNA accumulated mainly in microsporocytes and tapetum. By the time of anthesis, *ScFRK2* mRNA was no longer found in degenerating tapetum or pollen grains but instead found abundantly on the anther wall, including epidermis and endothecium. Overexpression of *ScFRK2* transcripts strongly disturbed pollen development. At maturity, almost two-thirds of pollen grains were severely affected and non-viable, while the remaining pollen grains were significantly smaller than wild type pollen. Cross with pollen from a *ScFRK2* overexpression line into a wild type female plant produced an F1 population with 44% of the progeny having the transgene, suggesting that the pollen defect is caused by a sporophytic dysfunction, leading to major structural defects and incomplete pollen development.

Keywords MAP kinase kinase kinase · Anther · Pollen · *Solanum chacoense*

Genbank accession number *ScFRK2* · AY427829

Abbreviations

DPA	Days post anthesis
FRK	Fertilization-related kinase
LRR	Leucine-rich repeat
MAPKKK	Mitogen-activated protein kinase kinase kinase
SEM	Scanning electron microscopy
TEM	Transmission electron microscopy

Introduction

Anthers produce the male gametes, the pollen grains, which are three-celled structures used for long distance fertilization. Pollen grains are generated through spore tetrads enclosed in a thick callose wall, which originate from another precursor: the sporogenous cell. The cell lineage that gives rise to the gametes and anther inner cell layers is more complex. At mid-anther development,

Martin O'Brien and Madoka Gray-Mitsumune contributed equally to this work.

M. O'Brien · M. Gray-Mitsumune · C. Kapfer · D. P. Matton (✉)
Institut de Recherche en Biologie Végétale (IRBV),
Département de sciences biologiques,
Université de Montréal, 4101 rue Sherbrooke est,
H1X 2B2 Montréal, QC, Canada
e-mail: dp.matton@umontreal.ca

C. Bertrand
Département d'Anatomie et Biologie Cellulaire,
Université de Sherbrooke, 3001 12ème Avenue Nord,
J1H 5N4 Sherbrroke, QC, Canada

archesporial initials arise from the L2 layer and divide periclinally to form a primary sporogenous cell facing inward and a parietal cell facing outside. The primary sporogenous cell is the precursor of the tetrad, while the primary parietal cell makes another periclinal division to yield an inner and an outer secondary parietal cell. The outer cells develop further to form the endothecium cell layer that will later play a role in pollen dehydration. The inner parietal cells divide once more periclinally and form a layer of tapetum cells and a middle cell layer that borders the endothecium and the tapetum (Bowman 1994; Scott et al. 2004). The tapetum is the nutritive layer of cells that lines the locule containing the developing microsporocytes. The microspores embedded in each tetrad are freed from one another by the action of callase, an enzyme produced by the tapetum. In later development stages, the tapetum cell layer degenerates, leaving an empty space filled with the enlarging microspores that will in time, each divide asymmetrically to give rise to a bicellular pollen grain where each of the two cells has its own developmental fate (Scott et al. 2004). Upon shedding, pollen grains are freed from the anther in a dehydrated form. The larger cell of the pollen grain, the vegetative cell, will form the pollen tube when pollen grain hydration occurs on the style's stigma. The smaller cell is found within the vegetative cell cytoplasm and is called the generative cell. The generative cell will undergo mitosis once more to produce two identical sperm cells (Boavida et al. 2005). In most species, including solanaceous plants, this second mitosis occurs during pollen tube growth in the gynoecium. Both sperm cells will be released from the pollen tube upon ovule fertilization. One will fuse with the egg cell to produce the zygote and the other one will fuse with the diploid central cell to generate the triploid endosperm, a process called double fertilization (Esau 1977). Stamen and pollen development has been recently reviewed in Scott et al. (2004).

Most of the mutations described that affect anthers or pollen have been shown to disturb either gamete meiosis, mitosis or chromosome partitioning (recently reviewed in Ma 2005; Wilson and Yang 2004). Fewer male defects are known to affect other processes such as anther development or pollen tube germination and growth. Multiple reports link protein kinases to different processes in anther and pollen biology. The *EXCESS MICROSPOROCYTES 1/EXTRA SPORONGENOUS CELLS* (*EMS1/EXS*) gene codes for a LRR receptor kinase in *Arabidopsis thaliana* and is involved in determination of anther cell fate (Canales et al. 2002; Zhao et al. 2002). In the *ems1/exs* mutant, more sporogenous cells are produced, which are derived from the incorrect cell fate acquisition of the middle cell and tapetum cell layers. The numerous microsporocytes in *ems1/exs* mutants degenerate either during (Zhao et al. 2002) or after (Canales et al. 2002) meiosis, resulting in complete pollen sterility. The pollen defect could be attributed to the absence of the nutritive tapetum cell layer. A mutation in *MULTIPLE SPOROCYTE 1* (*MSP1*) a rice ortholog of *EMS1*/EXS also results in similar defects (Nonomura et al. 2003). The *Zea mays multiple archesporial cells1* (*mac1*) mutant also shares some phenotypic features with *ems1/exs* and *msp1* mutations, although the identity of the gene is not yet known (Sheridan et al. 1999). The *exs/ems1* and *msp1* mutants also affect female gametophyte development (Nonomura et al. 2003) as well as endosperm and embryo development after fertilization (Canales et al. 2002). Similarly, the *tapetum determinant 1* (*tpd1*) mutant exhibits male defects apparently identical to the phenotype of the *exs/ems1/msp1* mutants (Yang et al. 2003). The protein encoded by the *TPD1* gene has no known function but it is secreted and has been hypothesized to act as a protein ligand for these receptors (Scott et al. 2004). Recently, the double knockout of *serk1/serk2* was shown to affect the cell determinacy of tapetum cells by conversion to microsporocytes, which will in time lead to pollen abortion and male sterility (Albrecht et al. 2005; Colcombet et al. 2005). The SERK1/2 LRR receptor kinases affect anther development in a similar way to EMS1/EXS. SERK1 overexpression was earlier shown to enhance the potential of suspension cultured cells to undergo somatic embryogenesis (Hecht et al. 2001; Schmidt et al. 1997), suggesting different functions of these receptors on different tissues. Finally, another class of LRR receptor kinases BAM1 and BAM2 have been shown to be involved in the differentiation of L2 layer cells (Hord et al. 2006). The double knockout of *bam1/bam2* lacks the endothecium, middle and tapetum layers, and instead forms cells resembling pollen mother cells. Similar to the *ems1/exs* mutants, the pollen mother cells degenerate during meiosis. Further gene expression analyses using these mutants suggested that BAM1/BAM2 pathway may work upstream of the EMS1/EXS pathway (Hord et al. 2006).

Other receptor kinases such as the *Lycopersicum esculentum* LePRK2 and the *Petunia inflata* PRK1 have been shown to be involved in pollen tube growth and microspore formation, respectively. The extracellular domain of LePRK2 interacts with LAT52, a cysteine-rich protein secreted from pollen (Tang et al. 2002). LAT52 is found abundantly in pollen and antisense inhibition of *LAT52* gene causes defects in pollen hydration and pollen tube growth, leading to male ste-

rility (Muschietti et al. 1994). Since both LePRK2 and LAT52 are found in pollen, LePRK2 and LAT52 binding may be part of an autocrine signaling pathway involved in the initiation and maintenance of pollen tube growth (Johnson and Preuss 2003). The *Petunia PRK1* was originally isolated from pollen but was later shown to be involved in development of both microspore and embryo sac. Down-regulation of *PRK1* causes microspores to halt their development at the uninucleate stage (Lee et al. 1996), while in the embryo sac, the two polar nuclei fail to migrate and fuse to form the central cell (Lee et al. 1997). Sucrose non-fermenting-1-related kinase (snRK1) from *Hordeum vulgare* is another kinase whose gene expression is specific to anther and pollen (Zhang et al. 2001). In the primary transformants of *snRK1* antisense lines, half the pollen grains have their development stopped at the binucleate stage. The *snRK1* transgene is not transmitted through the next generation by the pollen, indicating that the effect is gametophytic (Zhang et al. 2001).

We have recently shown that the ScFRK2 MAP kinase kinase kinase is involved in seed and fruit development and, when overexpressed, produces a homeotic conversion of ovules into carpelloid structures. While it is predominantly expressed in ovules, the *ScFRK2* is also expressed at significant levels in anthers (Gray-Mitsumune et al. 2006). In the present study, we analyzed in detail the defects that affect pollen grain and pollen development in transgenic plants overexpressing *ScFRK2*.

Materials and methods

Plant material and F1 population generation

The diploid and self-incompatible wild potato *Solanum chacoense* Bitt. ($2n = 2x = 24$) was grown in a greenhouse with 14–16 h of light per day. The genotype used for *Agrobacterium tumefaciens*-mediated transformation was G4 (self-incompatibility alleles S_{12} and S_{14}). One of the *ScFRK2* overexpression (*ScFRK2*-OX) lines showing pollen defects was crossed to a fully compatible *S. chacoense* plant genotype V22 (self-incompatibility alleles S_{11} and S_{13}) as female or male progenitor. Embryo rescue was performed to accelerate the production of the F1 generations in the reciprocal crosses. Twenty days after pollination, fruits were sterilized in a solution containing 10% sodium hypochlorite and 0.1% Tween 20 for 10 min. Fruits were then dissected to isolate fertilized ovules, which were then further dissected under a stereomicroscope in order to obtain intact embryos. Nineteen embryos were rescued for both populations. Embryos were individually grown in 0.5 × MS media until a 10 cm seedling was obtained. Plantlets were then transferred to the greenhouse for further analysis or used as such for DNA extraction.

DNA extraction and PCR analysis

Genomic DNA from leaf tissues of untransformed plants, transgenic plants and from the F1 populations was extracted with the DNeasy Plant Mini Kit (Qiagen, Mississauga, ON, Canada). To test the transmission of the T-DNA, PCR reactions were performed using 100 ng genomic DNA as a template and using three different primer pairs. Kan-F: 5′-GTCATTTCGAACC CCAGAGTC-3′ and Kan-R: 5′-CTGAATGAACTG CAGGACGAG-3′were used to amplify the kanamycin resistance gene; Nos1: 5′-CCCGATCTAGTAACAT AGATGACACC-3′ and Nos2: 5′-GAGATCTAGAT CGTTCAAACATTTGGCAATAAAG-3′were used to amplify the NOS terminator; CaMV35S-Pro: 5′-CT CCACTGACGTAAGGGATG-3′ and a *ScFRK2* gene specific primer SV2-C7-1: 5′-CTTTCTTCCCAGTAA TCATC-3′were used to amplify the exogenous *ScFRK2* gene. PCR products were separated in a 1% agarose gel and DNA bands were detected using ethidium bromide.

RNA isolation and analysis

RNA extraction of anther tissues was conducted as described previously (Jones et al. 1985). Ten μg RNA was separated in a formaldehyde/MOPS gel, then transferred to Hybond N+ membrane (GE Healthcare, Baie d'Urfée, QC, Canada), and crosslinked by UV (120 mJ/cm^2). To confirm equal loading between RNA samples, a 1 kb fragment of *S. chacoense 18S* RNA was PCR amplified and used as a control probe. Prehybridization was performed at 45°C for 3 h in a hybridization solution containing 50% deionized formamide, 6× SSC, 5× Denhardt's solution, 0.5% SDS and 200 μg/μl denatured salmon DNA. Hybridization of the membranes were performed overnight at 45°C in the same solution containing an appropriate probe. The α-^{32}P labeled probe for *ScFRK2* was synthesized using a full-length cDNA by the Strip-EZ DNA labeling kit (Ambion, Austin, TX, USA). Following hybridizations, membranes were washed three times in a solution containing 2× SSC and 0.1% SDS (30 min at 25°C, 30 min at 35°C; 30 min at 45°C), once in 1× SSC and 0.1% SDS (30 min at 55°C), and finally in 0.1× SSC and 0.1% SDS (10 min at 55°C). For *18S* rRNA hybridization, the last wash was repeated twice (30 min

at 55°C) for thorough removal of unbound probes. Blots were stripped following the manufacturer's instructions (Ambion). Signals were detected by exposing on Kodak Biomax MR film (Interscience, Markham, ON, Canada) at −86°C or on a Kodak storage phosphor screen followed by visualization in Typhoon™ 9200 imager (GE Healthcare).

In situ hybridization

Anthers were fixed in FAA (50% ethanol, 5% acetic acid, 1.85% formaldehyde) at 4°C overnight. They were then dehydrated in ethanol series, replaced by *tert*-butyl alcohol and embedded in paraffin. Ten µm sections were mounted on slides treated with 3-aminopropyltriethoxy-silane (Sigma, Oakville, ON, Canada) and in situ RNA hybridization was performed as described previously (Lantin et al. 1999). Sense and anti-sense digoxigenin-11-UTP labeled riboprobes were synthesized from a full-length *ScFRK2* cDNA using T3 and T7 RNA polymerases (Roche Diagnostics, Laval, QC, Canada). Probe concentration in the hybridization solution ranged from 0.1 to 0.5 ng/l. Sections were observed in a light microscope and digitally photographed using a Leica DFC420 Fire Cam.

Pollen viability and callose staining

For viability test, fresh pollen grains were suspended in a drop of 1% aceto-carmine and stained for 2 min on a slide. Pollen viability was scored by light microscopy of 3–12 different optical fields and photographed with an Olympus BHT microscope on Kodak Ektachrome 160T film. For callose staining, pollen was stained for 15 min in 0.1% aniline blue and observed in a Nikon Eclipse TE2000-U inverted microscope using UV light emission. Digital images were obtained using a CoolSnap fx camera (Photometrics, Tucson, AZ, USA) and analyzed using Image-Pro 3DS software (Media Cybernetics, Silver Spring, MD, USA).

Electron microscopy

For scanning electron microscopy (SEM), pollen grains were harvested manually by shaking and critical-point-dried with CO_2 without prior fixation and dehydration. Pollen grains were coated with gold-palladium, and viewed in a JEOL 840 scanning electron microscope at 10 kV. For pollen viability estimation through outer structure analysis, fresh pollen was observed with a Hitachi S-3000N variable pressure SEM at 30 Pa and 15 kV. For transmission electron microscopy (TEM), samples were fixed in 2.5% glutaraldehyde in sodium cacodylate buffer 0.1M pH 7.4, post-fixed in 2% osmium tetroxyde (OsO_4) in the same buffer, dehydrated in ethanol and embedded in Spurr's resin. Observations were made on a Hitachi H-7500 microscope. Statistics for pollen defects observed by SEM were scored from ≥100 pollen grains per wild type or transgenic lines.

Results

ScFRK2 mRNA expression in anthers

Since *ScFRK2* mRNAs had been previously shown to be expressed in anthers (Gray-Mitsumune et al. 2006), anthers from different developmental stages were collected and RNA levels were determined by RNA gel blot analysis (Fig. 1a). *ScFRK2* mRNA abundance remained constant in anthers until 3 days post anthesis (DPA). However, the *ScFRK2* mRNA levels increased markedly in anthers 4 and 5 DPA when anther dehiscence occurred. As for hybridization in other tissues, two nearly equimolar bands with identical expression pattern can be observed, most probably the result of the co-expression of a highly similar gene family member (Gray-Mitsumune et al. 2006). Equal RNA loading was verified by re-probing the stripped membrane with an *18S* RNA probe (Fig. 1a, lower panel).

To define *ScFRK2* mRNA localization, we conducted in situ RNA hybridizations on anthers at different developmental stages (Fig. 1b). In stage-2 anthers (stages defined as in Koltunow et al. 1990), a strong *ScFRK2* mRNA signal was detected in microsporocytes and signals in the other anther tissues were weak (Fig. 1b, ii and iii). As anthers developed, the *ScFRK2* mRNA signals became stronger in the tapetum while retaining strong signals in microsporocytes undergoing meiosis (data not shown). In stage 1 anthers, hybridization signals in the tapetum and tetrads were about the same while signals in the anther wall remained weak (Fig. 1b, v and vi). However, by the time of anthesis, *ScFRK2* mRNA signals were no longer detected in the degenerating tapetum layer or pollen grains (Fig. 1b, viii and ix). Instead, strong signals were detected in the anther wall, including epidermis, and endothecium cells (Fig. 1b, viii and ix). The stomium, vasculature and most of the connective tissues were devoid of *ScFRK2* transcripts (Fig. 1b, viii and ix). Sense probe hybridizations (Fig. 1b, i, iv. and vii) confirmed the specificity of the antisense *ScFRK2* probe. Light brown staining in the pollen and cell wall was detected in both sense and antisense probe hybridizations and, therefore considered an artifact.

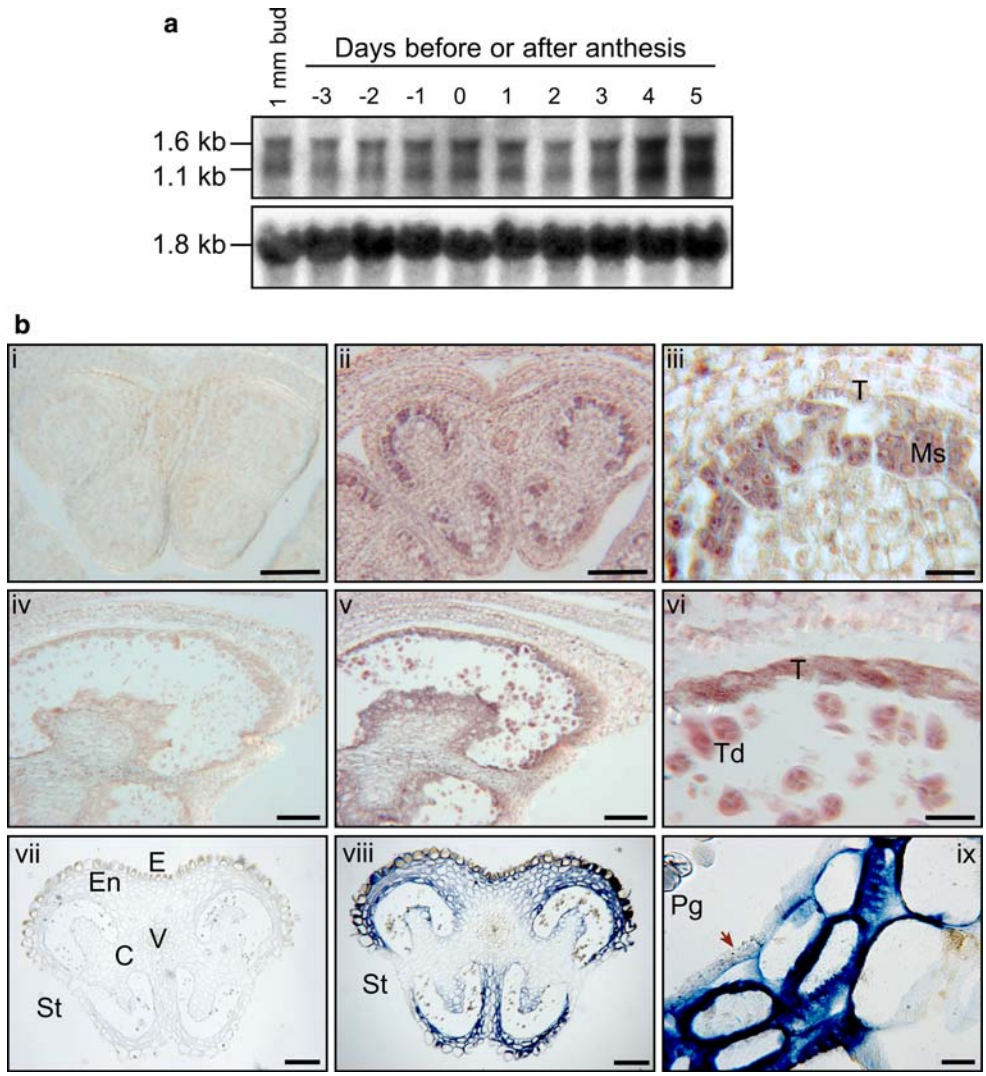

Fig. 1 Expression analysis of *ScFRK2* in anthers of *S. chacoense*. **a** RNA gel blot analysis of *ScFRK2* mRNA accumulation in anther tissues harvested in 1 mm length flower buds or from 3 days before anthesis to 5 days after anthesis. 10 μg of total RNA from the various tissues was detected using a probe against the full-length *ScFRK2* mRNA (*upper panel*). The RNA gel blot was stripped and re-hybridized using a probe against *18S* rRNA to ensure equal loading of the samples (*lower panel*). **b** In situ localization of *ScFRK2* transcripts in wild type anthers. Since early anther development of *Solanum* species is similar to tobacco, we adapted developmental stages of anther defined by Koltunow et al. (1990). Hybridization signals are seen as *bluish purple* staining. i, ii, and iii, Cross sections of a stage -2 anther. Sections were taken from a flower bud 1 mm in length. i Sense probe. ii and iii Antisense probe. iii Enlargement of ii showing the microsporocyte (*Ms*) and tapetum (*T*). iv, v and vi Oblique sections of a stage 1 anther. Sections were taken from a flower bud ~2.5–3.0 mm in length. iv Sense probe; v and vi Antisense probe. vi Enlargement of v showing the tetrad (*Td*) and tapetum (*T*). vii, viii and ix Cross sections of anther at anthesis. vii Sense probe. vii and ix Antisense probe. Magnification of the anther wall cell layers showing the degenerating outer tapetum area (*red arrow*). Scale bars, 250 μm (vii and viii); 100 μm (i, ii, iv, and v); 20 μm (iii, vi, and ix). *C* connective tissue, *E* epidermis, *En* endothecium, *Ms* microsporocyte, *Pg* pollen grain, *St* stomium, *T* tapetum, *Td* tetrad, *V* vasculature

Pollen defects in *ScFRK2* transgenic plants

Overexpressing lines of *ScFRK2* (*ScFRK2*-OX) show a homeotic conversion of ovules into carpelloid structures while antisense lines show no obvious phenotypes, possibly because of functional redundancy shared with other *MAPKKK* genes (Gray-Mitsumune et al. 2006). We used these overexpression lines to determine if there were also developmental defects in stamens, since this was the only other organ where significant expression of *ScFRK2* mRNAs could be observed. At the macroscopic level, no defects could be observed in *ScFRK2*-OX lines. Vegetative growth of transgenic plants appeared identical to that of wild type plants. Overall anther morphology as well as the timing of anther dehiscence also appeared normal. However, examination of pollen stained with 1% aceto-carmine revealed defects in pollen development.

With this staining, viable pollen grains are lightly stained in pink, while dead pollen cells are shown as empty and shriveled shells (Fig. 2g and h). At anthesis, anthers from *ScFRK2*-OX lines contained 30–50% dead pollen (Table 1 and Fig. 2h) while the wild type and a transgenic line with no detectable transgene expression showed very low (<0.5%) pollen lethality (Table 1 and Fig. 2g). To determine the timing of pollen lethality, we examined viability of pollen/microspore at different stages of maturity (Fig. 2a to h). At the tetrad and uninucleate stages, no microspore defects were detected in *ScFRK2*-OX plants (Fig. 2b). However, *ScFRK2*-OX lines showed a steady increase in pollen lethality as pollen matured (Fig. 2f and h). Pollen lethality was first detected around 3 days prior to anthesis (Fig. 2f). *ScFRK2* lines S1 and S2 exhibited pollen lethality of 11.9 ± 1.2% and 17.2 ± 1.7% respectively, at 3 days prior to anthesis; 38.8 ± 2.7% and 36.1 ± 3.4% respectively, at 1 day prior to anthesis; and 49.3 ± 5.9% and 47.4 ± 0.8% respectively, at anthesis (Fig. 2h). After anthesis, the proportion of dead pollen remained constant (52.8 ± 6.9% and 47.2 ± 1.2% at 5 DPA). Wild type pollen exhibited no significant lethality throughout the different stages observed (Fig. 2a, c, e and g).

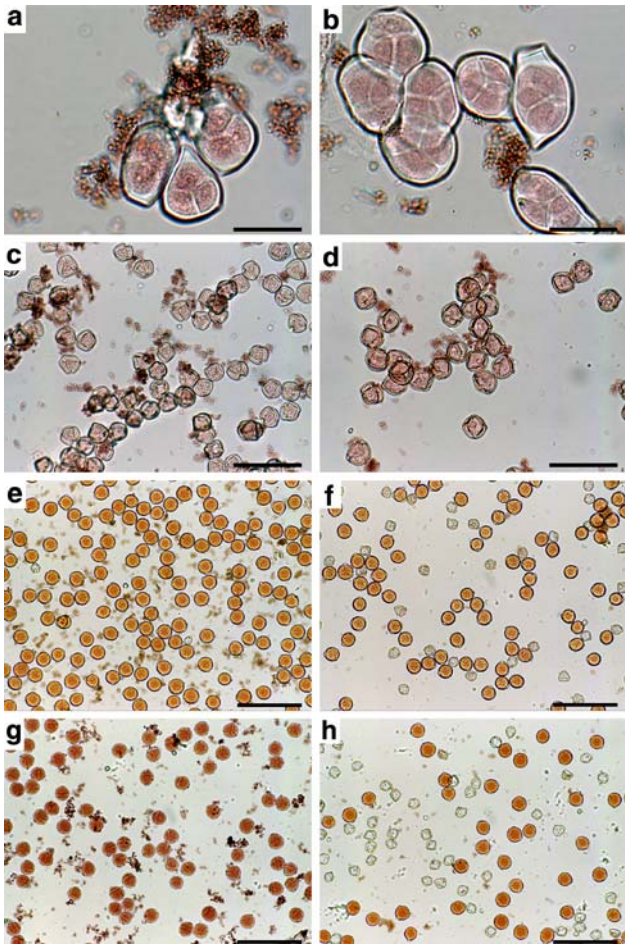

Fig. 2 Pollen viability in wild type and *ScFRK2*-OX plants. Pollen was stained with 1% aceto-carmine. Viable pollen grains are lightly stained in *pink*, while dead pollen cells are shown as empty and shriveled shells. **a**, **c**, **e** and **g** Wild type plant. **b**, **d**, **f** and **h** *ScFRK2*–OX line S2. **a** and **b** Tetrads. **c** and **d** Uninucleate microspores. **e** and **f** Pollen 3 days prior to anthesis. **g** and **h** Pollen at anthesis. Scale bars, 20 μm (**a** and **b**); 50 μm (**c** and **d**); 80 μm (**e**–**h**)

Table 1 Mean percentage of pollen lethality in primary transformants carrying a *35S::ScFRK2 transgene*

Plant genotype	Pollen lethality (%)
WT *S. chacoense*	0.5
ScFRK2-OX line S1	55.2
ScFRK2-OX line S2	48.3
ScFRK2-OX line S8	31.5
ScFRK2-OX line S14	42.1
ScFRK2-OX line S16	49.2
ScFRK2-OX line S17	44.6
ScFRK2-OX line S3[a]	0.1

Pollen lethality was scored in pollen stained with 1% aceto-carmine. Overexpression of *ScFRK2* was confirmed by RNA blotting (data not shown)

[a] *ScFRK2*-OX line S3 is used as a control transgenic line that showed no detectable overexpression of the *ScFRK2* transgene

To analyze the pollen defects of the *ScFRK2*-OX lines in more detail, pollen grains were observed by scanning electron microscopy (SEM). Wild type plants showed typical tricolpate pollen grains with three equally distributed apertures that run longitudinally to the pollen axis (Fig. 3a). The pollen grain appearance is different from that of light microscopy (Fig. 2a), since aceto-carmine staining causes water uptake and hydration of the pollen grain, thus taking a spherical shape. For this reason, aceto-carmine staining tends to underestimate pollen defects. In fact, SEM analysis revealed defects in more than 50% of the pollen grains. Dead pollen grains appeared shriveled, leaving the impression of empty collapsed shells (Fig. 3b). The proportion of shriveled pollen grains according to SEM analysis was 4.3 ± 2.8% for wild type and 62.4 ± 1.9% for the *ScFRK2*-OX S2 line. In addition to shriveled pollen, the S2 line contained slightly odd-shaped pollen grains, which could not be detected in aceto-carmine staining (data not shown).

Close observations of the pollen wall in SEM showed identical sexine patterning (the sculptured outer layer of the exine) for both wild type and shriveled S2 pollen grains (Fig. 3c and d), suggesting that the defect is not related to sporopollenin deposition. Similarly, callose staining using aniline blue, revealed no significant differences in cell wall callose deposition between wild type and shriveled S2 pollen (Fig. 3e and f). In wild type

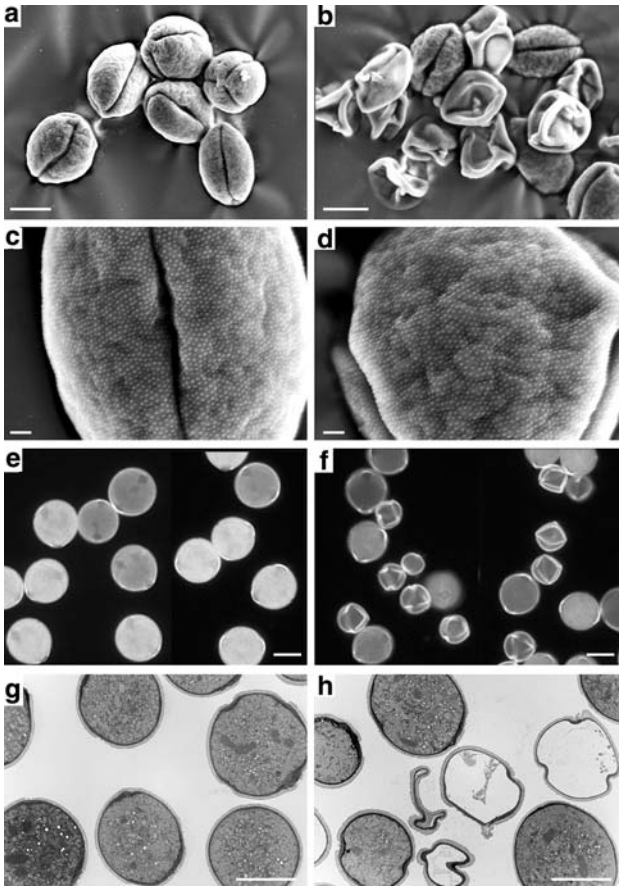

Fig. 3 Examination of pollen outer structures. For all analyses, pollen was harvested at the time of anthesis. **a** SEM of wild type pollen. **b** SEM of *ScFRK2*-OX S2 pollen. **c** SEM of wild type pollen showing the sexine. **d** SEM of *ScFRK2*-OX S2 pollen showing the sexine. **e** Callose staining with aniline blue of wild type pollen. **f** Callose staining with aniline blue of *ScFRK2*-OX S2 pollen. **g** TEM of wild type pollen. **h** TEM of *ScFRK2*-OX S2 pollen. Scale bars, 10 μm (**a**, **b**, **e**–**h**); 1 μm (**c** and **d**)

pollen, callose deposition was detected strongly around apertures and more diffusely throughout the cell wall (Fig. 3e). A similar staining pattern was also seen in normal-looking pollen in S2 plants (Fig. 3f). In the shriveled S2 pollen, callose is detected on all ridges but overall callose deposition was similar to the level observed in wild type pollen (Fig. 3f). Furthermore, examination under a transmission electron microscope (TEM) confirmed proper cell wall deposition in shriveled S2 pollen grains (Fig. 3h, and data not shown).

Since the callose staining was performed in a pollen hydration media, it was possible to compare pollen sizes between wild type and mutant plants. Grain sizes were compared using arbitrary units (au) determined by pixel filling of entire pollen grain contour. *ScFRK2*-OX S2 plants contained two populations of pollen grains, normal and shriveled. Naturally, shriveled *ScFRK2*-OX S2 pollen grains were considerably smaller, reaching only 40% (17.0 ± 1.3 au, $n = 20$) of wild type grains. Normal-looking pollen grains from S2 plants were also significantly smaller (32.2 ± 3.7 au, $n = 20$) than wild type (42.1 ± 2.2 au, $n = 20$), reaching only 76% of wild type pollen grains, indicating that *ScFRK2* overexpression affected the entire population of pollen grains. Although normal-looking pollen grains in S2 plants were smaller than wild type pollen grains, TEM images revealed no significant differences in the cellular ultrastructure between the two types of pollen grains (Fig. 3g and h, and data not shown). These normal-looking S2 pollen grains also appeared functional, as they were able to pollinate and fertilize wild type plants and produce progenies (see below).

F1 population analysis

Pollen development defects can be of either sporophytic or gametophytic origin. To distinguish between these two possibilities, we studied the transgene transmission to the successive generation. We used the *ScFRK2*-OX line S2, harboring a single T-DNA insertion (data not shown). In a primary transformant, only half the pollen grains should carry the transgene. We collected the *ScFRK2*-S2 pollen and crossed it to fully compatible *S. chacoense* wild type genotype V22 as female progenitor. If the defect was caused by a gametophytic dysfunction, the transmission of the transgene to the F1 generation would have been greatly reduced. However, 44% (7/16) of F1 progenies scored positive for both kanamycin resistance and *35S::ScFRK2* genes, which is not significantly different from the expected value for Mendelian inheritance (50%). Therefore, this suggests that the observed pollen defect resulted from sporophytic dysfunction.

To further confirm that the observed pollen phenotype was due to *ScFRK2* overexpression and not due to a mutation caused by the T-DNA insertion, we generated a F1 population from a cross between a wild type V22 plant as the pollen donor and the *ScFRK2*-OX line S2 as the female progenitor. Wild type V22 was used as the pollen donor to ensure that the population generated was not biased by a male parent already showing a pollen defect. Out of 19 F1 progenies analyzed, 11 exhibited higher *ScFRK2* transcript levels than the untransformed control and, therefore, were kept for further analyses. These selected individuals were grouped into three categories of *ScFRK2* expression levels and compared with the severity of the pollen defects as estimated by aceto-carmine staining. As *ScFRK2* mRNA levels increased, pollen lethality followed accordingly, thus establishing a direct link between *ScFRK2* overexpression and the pollen defect (Fig. 4). The homeotic change

of ovules shown previously (Gray-Mitsumune et al. 2006) was also transmitted to this population but less frequently (or less severely) than the pollen phenotype (data not shown). This may be due to differences in ScFRK2 interacting partners and downstream targets between the two tissues. The effect on these partners or targets may also have different thresholds depending of the *ScFRK2* overexpression level.

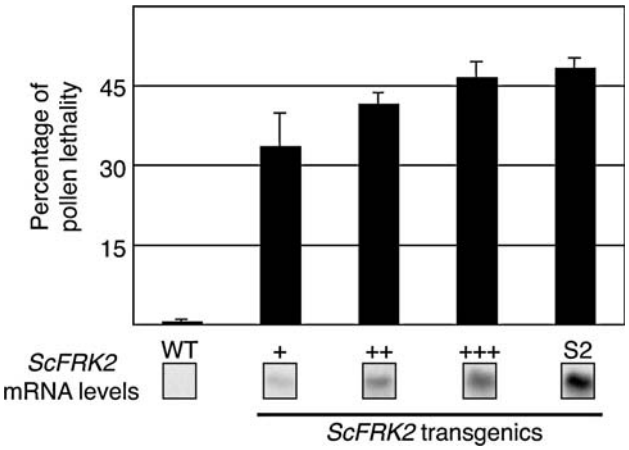

Fig. 4 Pollen lethality correlates with *ScFRK2* transcript abundance. F1 population produced from the *ScFRK2*-OX line S2 as the female progenitor (S alleles $S_{12}S_{14}$) and a wild type plant genotype V22 (S alleles $S_{11}S_{13}$) as the pollen donor, was divided into three categories of *ScFRK2* mRNA expression levels. For the RNA gel blot analysis, in order to clearly show the differences between the various levels of overexpression, an exposure of 1 day was used instead of the 4 days needed to reveal the wild type expression of the *ScFRK2* gene. The number of progenies for each category was as follows: +, $n = 4$; ++, $n = 5$; +++, $n = 2$. The bar represents average pollen lethality ± standard deviation

Tissue distribution of *ScFRK2* mRNA in *ScFRK2*-OX anthers

In situ RNA hybridization analysis was performed to determine the tissue distribution of *ScFRK2* mRNAs in *ScFRK2*-OX S2 plants (Fig. 5). Hybridization of wild type and S2 anthers was performed simultaneously using identical conditions to allow direct comparison. It should be noted that the staining in wild type sections appears much weaker than that shown in Fig. 1b because color development was stopped earlier to avoid saturation in S2 anthers. In situ RNA hybridization confirmed the overexpression of *ScFRK2* in all the tissue types of developing S2 anther, including tapetum, microsporocyte, epidermis, endothecium, connective tissue and vasculature (Fig. 5c). Yet, *ScFRK2* mRNA was more abundant in the tissues where the gene is normally expressed, the tapetum and microsporocytes (Fig. 5c and f). This suggests, as observed before in female reproductive organs (Gray-Mitsumune et al. 2006), that regulatory elements driving proper tissue-specific expression are most probably present in the *ScFRK2* transcribed region.

Discussion

Signal transduction is at the heart of every life process and protein kinases, enzymes capable of modifying other proteins by adding phosphate groups, are key regulators for signaling events. Phosphorylation usually results in a functional change of the target protein

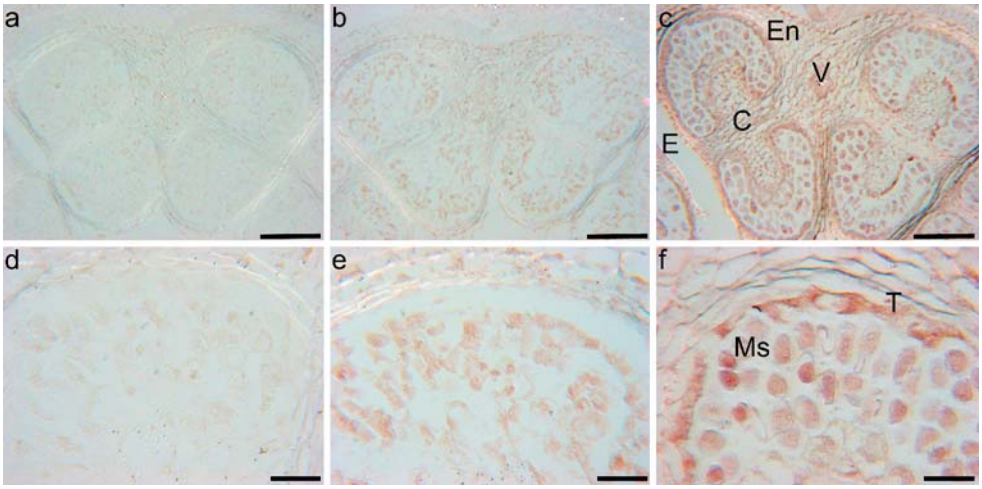

Fig. 5 Comparison of *ScFRK2* mRNA distribution between wild type and *ScFRK2*-OX S2 anthers. In situ RNA hybridization was performed simultaneously using identical conditions to allow direct comparisons between wild type and transgenic plants. Color development of in situ signals were stopped earlier than those shown in Fig. 1 to avoid color saturation. Shown are cross sections of stage -1 anthers. Sections were taken from flower buds ~2 mm in length. **a** Wild type anther, sense probe. **b** Wild type anther, antisense probe. **c** S2 anther, antisense probe. **d**, **e** and **f** Enlargement of **a**, **b** and **c**, respectively. Scale bars, 100 μm (**a**–**c**); 20 μm (**d**–**f**). *C* connective tissue; *E* epidermis; *En* endothecium; *Ms* microsporocyte; *T* tapetum

or substrate, either by changing its activity, cellular location or association with other proteins. In order to gain information about protein kinases acting during plant fertilization and embryogenesis, we used a reverse genetic approach to determine the role of protein kinases expressed in reproductive tissues (Germain et al. 2005). Out of an EST library normalized for weakly expressed genes in fertilized ovaries, we isolated two genes named *ScFRK1* and *ScFRK2* (*Solanum chacoense* Fertilization-Related Kinase 1 and 2) that belonged to the MAPKKK MEKK subfamily (Gray-Mitsumune et al. 2006). Of all the tissues tested, *ScFRK2* is most strongly expressed in anthers, styles and in fertilized ovules. We have previously shown that *ScFRK2* is involved in ovule and seed development (Gray-Mitsumune et al. 2006). The present study shows that *ScFRK2* is also involved in anther development.

ScFRK2 mRNA levels detected by RNA gel blot analysis were relatively constant during early and mid-anther development (Fig. 1a). Yet, there was a dramatic change in tissue distribution of *ScFRK2* mRNA when detected by in situ RNA hybridization (Fig. 1b). During early anther development, *ScFRK2* mRNA was detected in the microsporocytes, the progenitor of the male gametophytes (Fig. 1b, ii). As the anther developed, stronger *ScFRK2* mRNA was detected in sporophytic tissue, first in the tapetum (Fig. 1b, vi), and then, after tapetum degeneration, in the epidermis and endothecium (Fig. 1b, viii), while pollen grains, the male gametophyte, contained little *ScFRK2* mRNA (Fig. 1b, ix). These changes in *ScFRK2* mRNA distribution suggest that *ScFRK2* has multiple functions in anther development and is involved in the development of both gametophytic and sporophytic tissue of the anther.

Although ectopic expression can sometime lead to pleiotropic effects on plant development, phenotypic abnormalities were found only in developing ovaries (Gray-Mitsumune et al. 2006) and anthers (this study), where *ScFRK2* was most strongly expressed during normal development. This suggests that the ScFRK2 kinase acts only on the cells that contain its cognate signaling pathway partners and targets. Ectopic expression of *ScFRK2* in the anther tissues normally devoid of the transcript, such as connective tissues, stomium and vasculature, did not cause defects in anther dehiscence. Instead, *ScFRK2*-OX plants exhibited variable degrees of pollen lethality, depending on the strength of *ScFRK2* overexpression (Table 1, Fig. 4). Initial assessment of pollen lethality suggested that the observed defects were of gametophytic origin, because pollen lethality detected by aceto-carmine staining did not exceed 50% (Table 1). However, a careful observation by SEM revealed that almost two thirds (62.4%) of pollen grains were shriveled (Fig. 3a). Furthermore, even those that appeared of normal shape were significantly smaller than wild type pollen grains, suggesting that almost all pollen grains in transgenic plants were affected to some degree. These observations cannot be explained by a gametophytic dysfunction since only half of the pollen grain population should carry the transgene. Instead, they suggest sporophytic dysfunction of *ScFRK2*-OX anthers. To determine the origin of *ScFRK2*-OX pollen defects, a wild type female progenitor plant was pollinated with *ScFRK2*-OX pollen. In the resulting F1 population, about half the plants (7/16) carried the transgene, a ratio expected in Mendelian inheritance. Therefore, we determined that the pollen defect caused by *ScFRK2* overexpression mainly originated from a sporophytic dysfunction.

If pollen lethality is caused by a sporophytic dysfunction, why were the individual pollen grains differently affected in the pollen population? One possible explanation for this may be due to the genetic variability found within the pollen grain population. Since *Solanum chacoense* is a self-incompatible species, heterozygosity is expected to be very high, hence an increase in interpollen genetic variability. Also, it should be noted that pollen defects caused by sporophytic dysfunctions do not always result in 100% pollen lethality. For example, in the *atmyb32* knockout mutant, homozygous lines display a partially male sterile phenotype with more than 50% aberrant pollen (Preston et al. 2004).

The accumulated evidences indicate sporophytic tissues, such as the tapetum and middle layer cells, to play key roles in supplying materials and signals essential for pollen development. The first line evidence for the critical function of the tapetum layer came from the genetic ablation study by Koltunow et al. (1990), where the tapetum-specific expression of the diphtheria toxin A-chain gene resulted not only in the destruction of the tapetum layer but also in the cessation of microsporogenesis and the subsequent degeneration of microsporocytes. Since then, several other mutations have been reported to cause pollen sterility due to aberrant development of the tapetum. In the *ems1/exs* (Canales et al. 2002; Zhao et al. 2002), *tpd1* (Yang et al. 2003), *serk1/serk2* (Albrecht et al. 2005; Colcombet et al. 2005), *msp* (Nonomura et al. 2003), *bam1/bam2* (Hord et al. 2006), and *mac1* (Sheridan et al. 1999) mutants described above, which lack the tapetum and acquire extra sporogenic cells instead, sporophytic dysfunction is detected during the pre-meiotic phase. A second class of mutants affects the tapetum during the post-meiotic phase. In

Arabidopsis mutants *male sterility 1* (*ms1*) (Wilson et al. 2001), *gus-negative 1* and *4* (*gne1, gne4*) (Sorensen et al. 2002), *aborted microspores* (*ams*) (Sorensen et al. 2003), *dysfunctional tapetum1* (*dyt1*) (Zhang et al. 2006), and the rice mutant *undeveloped tapetum1* (*udt1*) (Jung et al. 2005), all four layers of the anther wall are formed correctly, however, as microsporocytes undergo meiosis, the tapetum becomes vacuolated and enlarged, and subsequently the microspores become vacuolated and eventually degenerate. *MS1*, *AMS, DYT1*, and *UDT1* genes code for putative transcription factors, while the gene identities of *GNE1* and *GNE4* are not known. All of the mutants listed thus far causes severe pollen sterility and produce few, if any, functional pollen grains. In addition, sporophytic dysfunction is reflected by morphological changes to the tapetum cells. In the case of *ScFRK2*-OX plants, however, pollen sterility was never as severe and the tapetum appeared normal throughout the anther development (data not shown).

Pollen defects may be brought by more subtle mutations that do not cause morphological changes to the tapetum but impair tapetum functions. For example, in the knockout mutant of *Arabidopsis AtMYB32* transcription factor gene, the tapetum appears to develop and degenerate similarly as in the wild type plants, yet more than 50% of the pollen grains are shriveled and lack cytoplasm (Preston et al. 2004). Segregation analysis of mutant alleles showed that the pollen defect is caused by a sporophytic dysfunction. *AtMYB32* is normally expressed in the tapetum and may provide compounds, possibly derivatives from the phenylpropanoid pathway, which are required for proper pollen formation (Preston et al. 2004). The knockout mutant of *AtMYB4*, a gene closely related to *AtMYB32*, exhibits pollen defects similar to *atmyb32.* Interestingly, overexpression of *AtMYB4* also causes a similar but distinct pollen defect, possibly due to channeling the flux of different branches of the phenylpropanoid pathway (Preston et al. 2004). Although similarities between *atmyb32* mutant and *ScFRK2*-OX anthers are very interesting and it is tempting to make connection between the two pathways, this does not necessarily indicate that they may work in the same pathway. Instead, they represent a similar class of mutants whose tapetum function is impaired without major changes in the tapetum morphology. Progression of pollen lethality in *ScFRK2*-OX plants reached a plateau around the same time the tapetum degenerated (see text above), which is also consistent with impairment of tapetum function in *ScFRK2*.

Finally, one could not exclude the possibility that other tissues, such as the middle layer and endothecium, may contribute to sporophytic dysfunction of *ScFRK2*-OX anthers, although the involvement of these tissues in pollen development is obscure at this point. Wherever the defect may arise from, the trigger must be subtle such as changes in biochemical components. Yet, once initiated, it causes major structural defects and premature death of pollen grains. Our study illustrates yet another example in which the proper function of tapetum and/or endothecium plays a central role for pollen integrity and viability. Defining the involvement of *ScFRK2* in this process will help us understand the role of this protein kinase in a new signaling pathway involved in anther and pollen development.

Acknowledgments We thank Gabriel Téodorescu for plant care and maintenance. M. O'Brien is the recipient of Ph. D. fellowships from the Natural Sciences and Engineering Research Council of Canada (NSERC) and from Le Fonds Québécois de la Recherche sur la Nature et les Technologies (FQRNT, Québec), and C. Kapfer is the recipient of a M. Sc. fellowship from NSERC. D.P. Matton holds a Canada Research Chair in Functional Genomics and Plant Signal Transduction.

References

Albrecht C, Russinova E, Hecht V, Baaijens E, de Vries S (2005) The Arabidopsis thaliana SOMATIC EMBRYOGENESIS RECEPTOR-LIKE KINASES1 and 2 control male sporogenesis. Plant Cell 17:3337–3349

Boavida LC, Becker JD, Feijo JA (2005) The making of gametes in higher plants. Int J Dev Biol 49:595–614

Bowman J (1994) Arabidopsis: an atlas of morphology and development. Springer, Berlin Heidelberg New York

Canales C, Bhatt AM, Scott R, Dickinson H (2002) EXS, a putative LRR receptor kinase, regulates male germline cell number and tapetal identity and promotes seed development in Arabidopsis. Curr Biol 12:1718–1727

Colcombet J, Boisson-Dernier A, Ros-Palau R, Vera CE, Schroeder JI (2005) Arabidopsis SOMATIC EMBRYOGENESIS RECEPTOR KINASES1 and 2 are essential for tapetum development and microspore maturation. Plant Cell 17:3350–3361

Esau K (1977) Anatomy of seed plants. Wiley, New York

Germain H, Rudd S, Zotti C, Caron S, O'Brien M, Chantha SC, Lagace M, Major F, Matton DP (2005) A 6374 unigene set corresponding to low abundance transcripts expressed following fertilization in solanum chacoense bitt, and characterization of 30 receptor-like kinases. Plant Mol Biol 59:515–532

Gray-Mitsumune M, O'Brien M, Bertrand C, Tebbji F, Nantel A, Matton DP (2006) Loss of ovule identity induced by overexpression of the fertilization-related kinase 2 (ScFRK2), a MAPKKK from Solanum chacoense. J Exp Bot (In press). DOI 10.1093/jxb/erl194

Hecht V, Vielle-Calzada JP, Hartog MV, Schmidt ED, Boutilier K, Grossniklaus U, de Vries SC (2001) The Arabidopsis SOMATIC EMBRYOGENESIS RECEPTOR KINASE 1 gene is expressed in developing ovules and embryos and enhances embryogenic competence in culture. Plant Physiol 127:803–816

Hord CL, Chen C, Deyoung BJ, Clark SE, Ma H (2006) The BAM1/BAM2 receptor-like kinases are important regulators of Arabidopsis early anther development. Plant Cell 18:1667–1680

Johnson MA, Preuss D (2003) On your mark, get set, GROW! LePRK2-LAT52 interactions regulate pollen tube growth. Trends Plant Sci 8:97–99

Jones JDG, Dunsmuir P, Bedbrook J (1985) High level expression of introduced chimeric genes in regenerated transformed plants. EMBO J 4:2411–2418

Jung KH, Han MJ, Lee YS, Kim YW, Hwang I, Kim MJ, Kim YK, Nahm BH, An G (2005) Rice Undeveloped Tapetum1 is a major regulator of early tapetum development. Plant Cell 17:2705–2722

Koltunow AM, Truettner J, Cox KH, Wallroth M, Goldberg RB (1990) Different Temporal and Spatial Gene Expression Patterns Occur during Anther Development. Plant Cell 2:1201–1224

Lantin S, O'Brien M, Matton DP (1999) Pollination, wounding and jasmonate treatments induce the expression of a developmentally regulated pistil dioxygenase at a distance, in the ovary, in the wild potato Solanum chacoense Bitt. Plant Mol Biol 41:371–386

Lee HS, Karunanandaa B, McCubbin A, Gilroy S, Kao Th (1996) PRK1, a receptor-like kinase of Petunia inflata, is essential for postmeiotic development of pollen. Plant J 9:613–624

Lee HS, Chung YY, Das C, Karunanandaa B, van Went JL, Mariani C, Kao TH (1997) Embryo sac development is affected in *Petunia inflata* plants transformed with an antisense gene encoding the extracellular domain of receptor kinase PRK1. Sex Plant Reprod 10:341–350

Ma H (2005) Molecular genetic analyses of microsporogenesis and microgametogenesis in flowering plants. Annu Rev Plant Biol 56:393–434

Muschietti J, Dircks L, Vancanneyt G, McCormick S (1994) LAT52 protein is essential for tomato pollen development: pollen expressing antisense LAT52 RNA hydrates and germinates abnormally and cannot achieve fertilization. Plant J 6:321–338

Nonomura K, Miyoshi K, Eiguchi M, Suzuki T, Miyao A, Hirochika H, Kurata N (2003) The MSP1 gene is necessary to restrict the number of cells entering into male and female sporogenesis and to initiate anther wall formation in rice. Plant Cell 15:1728–1739

Preston J, Wheeler J, Heazlewood J, Li SF, Parish RW (2004) AtMYB32 is required for normal pollen development in Arabidopsis thaliana. Plant J 40:979–995

Schmidt ED, Guzzo F, Toonen MA, de Vries SC (1997) A leucine-rich repeat containing receptor-like kinase marks somatic plant cells competent to form embryos. Development 124:2049–2062

Scott RJ, Spielman M, Dickinson HG (2004) Stamen structure and function. Plant Cell Suppl(16):S46–S60

Sheridan WF, Golubeva EA, Abrhamova LI, Golubovskaya IN (1999) The mac1 mutation alters the developmental fate of the hypodermal cells and their cellular progeny in the maize anther. Genetics 153:933–941

Sorensen A, Guerineau F, Canales-Holzeis C, Dickinson HG, Scott RJ (2002) A novel extinction screen in Arabidopsis thaliana identifies mutant plants defective in early microsporangial development. Plant J 29:581–594

Sorensen AM, Krober S, Unte US, Huijser P, Dekker K, Saedler H (2003) The Arabidopsis ABORTED MICROSPORES (AMS) gene encodes a MYC class transcription factor. Plant J 33:413–423

Tang W, Ezcurra I, Muschietti J, McCormick S (2002) A cysteine-rich extracellular protein, LAT52, interacts with the extracellular domain of the pollen receptor kinase LePRK2. Plant Cell 14:2277–2287

Wilson ZA, Yang C (2004) Plant gametogenesis: conservation and contrasts in development. Reproduction 128:483–492

Wilson ZA, Morroll SM, Dawson J, Swarup R, Tighe PJ (2001) The arabidopsis MALE STERILITY1 (MS1) gene is a transcriptional regulator of male gametogenesis, with homology to the PHD-finger family of transcription factors. Plant J 28:27–39

Yang SL, Xie LF, Mao HZ, Puah CS, Yang WC, Jiang L, Sundaresan V, Ye D (2003) Tapetum determinant 1 is required for cell specialization in the arabidopsis anther. Plant Cell 15:2792–2804

Zhang Y, Shewry PR, Jones H, Barcelo P, Lazzeri PA, Halford NG (2001) Expression of antisense SnRK1 protein kinase sequence causes abnormal pollen development and male sterility in transgenic barley. Plant J 28:431–441

Zhang W, Sun Y, Timofejeva L, Chen C, Grossniklaus U, Ma H (2006) Regulation of arabidopsis tapetum development and function by DYSFUNCTIONAL TAPETUM1 (DYT1) encoding a putative bHLH transcription factor. Development 133:3085–3095

Zhao DZ, Wang GF, Speal B, Ma H (2002) The excess microsporocytes1 gene encodes a putative leucine-rich repeat receptor protein kinase that controls somatic and reproductive cell fates in the arabidopsis anther. Genes Dev 16:2021–2031